Vibrational Spectroscopy 139 (2025) 103818

Contents lists available at ScienceDirect

Vibrational Spectroscopy

journal homepage: www.elsevier.com/locate/vibspec

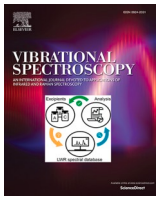

Vibrational spectroscopy as a tool for the investigation of polymer bases in motion picture films: A comparison between mid-infrared, near-infrared and Raman techniques

Alessia Buttarelli [a], Margherita Longoni [a], Valentina Rossetto [b], Silvia Bruni [a,*]

[a] Dipartimento di Chimica, Università degli Studi di Milano, via C. Golgi 19, Milano 20133, Italy
[b] Cineteca Nazionale, Centro Sperimentale di Cinematografia, Via Tuscolana 1524, Roma 00173, Italy

ARTICLE INFO

Keywords:
Reflection FTIR
Raman
NIR
Motion picture films
Polymers

ABSTRACT

In the present work, numerous samples of motion picture films from different brands and spanning a wide chronological range were examined with the aim of studying their polymeric support materials using various vibrational spectroscopic techniques. The bases of the films investigated included cellulose nitrate, cellulose acetate, polyethylene terephthalate (PET), and cellophane, the support material of the unique Ozaphan films. Regarding Fourier-transform infrared (FTIR) spectroscopy, the external reflection (ER) technique was employed, both in the mid-infrared (MIR) range and in the longer-wavelength portion of the near-infrared (NIR) region. For Raman spectroscopy, the sequentially shifted excitation (SSE™) technique was used to minimize issues related to potential fluorescence emission. The information provided by each technique was carefully considered, particularly in terms of penetration depth and specificity towards certain molecular structures. Furthermore, diffuse reflectance spectroscopy in the entire NIR range was combined with partial least squares (PLS) regression of the spectral data to estimate the degree of substitution (DS) of the polymer in cellulose acetate bases. This parameter is influenced both by the historical period in which the films were produced and possibly by degradation phenomena.

1. Introduction

The development of new cinematographic and photographic films was driven by humanity's need to capture reality on a tangible support, preserving it over time. This led to the creation of numerous types of support, initially for photography and, after the 1890s, for cinematography, which today constitute audiovisual heritage. The fragility and historical-artistic significance of these materials, combined with the growing debate between analog and digital restoration of audiovisual heritage, make a critical and preferably non-invasive study essential for their conservation and valorization.

The study of these materials is not always straightforward, since a cinematographic film is a complex system composed of various chemical components. Generally, the film consists of a polymeric base, which constitutes about 90 % of its structure, on which an emulsion layer is applied. This emulsion is responsible for the formation of the final image through the reduction of silver halides embedded in a binder, typically gelatin [1].

A high-quality film base must be flexible, transparent, wear resistant, non-flammable, and stable over time. The first polymer used for film production was celluloid, introduced in 1889 and derived from nitrocellulose and camphor. However, due to its high flammability and chemical instability, celluloid was gradually replaced by cellulose acetate, known as "safety film." In the 1920s, cellulose diacetate-based films were introduced, followed in the 1930s by cellulose triacetate [2]. Other mixed esters derived from cellulose acetate, such as cellulose acetate butyrate and cellulose acetate propionate, were also used as film supports.

Despite being labeled as "safety films," cellulose acetate films were still subject to degradation, including the notorious "vinegar syndrome", an autocatalytic process that produces acetic acid and ultimately leads to the deterioration of the film. Another common issue was the release of additives, such as plasticizers, onto the film surface. For these reasons, during the 1960s and 1970s, cellulose acetate was progressively replaced by polyester, a synthetic polymer that proved to be safer and more stable than cellulose derivatives. Two types of polyester have been

* Corresponding author.
E-mail address: silvia.bruni@unimi.it (S. Bruni).

https://doi.org/10.1016/j.vibspec.2025.103818
Received 21 February 2025; Received in revised form 19 May 2025; Accepted 29 May 2025
Available online 30 May 2025
0924-2031/© 2025 The Author(s). Published by Elsevier B.V. This is an open access article under the CC BY license (http://creativecommons.org/licenses/by/4.0/).

used in cinematographic films: polyethylene terephthalate (PET), the most used, and polyethylene naphthalate (PEN) [3].

As discussed in more detail below, alternative materials such as cellophane were also used as film supports for limited periods, employing a different method of producing an image.

The molecular structures of the various polymeric supports are shown in Fig. 1.

In light of the different chemical stability of materials used over the decades, understanding the specific polymer that forms the base of a cinematographic film is crucial for its correct conservation, as well as for the preservation of other films within a collection. In fact, the nitric or acetic acid produced during the deterioration of cellulose nitrate or cellulose acetate films [4] can also affect other materials stored nearby [5].

Regarding cellulose acetate supports, it is important to note that "cellulose acetate" is a generic term that refers to all products of the acetylation reaction between cellulose polymers and an excess of acetic anhydride, with sulfuric acid acting as a catalyst [6]. The physical and chemical properties of cellulose acetate depend on its degree of substitution (DS), which represents the average number of hydroxyl groups replaced by acetyl groups in each cellulose unit. From a preservation and storage perspective, knowing the DS of a film support provides valuable information, such as the approximate date of its production and its state of degradation. Hydrolysis, one of the main degradation mechanisms, causes a loss of acetyl groups, leading to a decrease in the DS of the polymer.

In principle, the edge printing on a film, which includes brand and code information, allows identification of the polymer base. However, such markings are not always present on older films or may be missing in cases where only fragments of the film have survived. For this reason, laboratories specialized in film conservation use alternative tests, most of which are destructive, such as treatments with specific reagents or even combustion. However, in addition to being destructive, these methods are not always reliable, especially when dealing with deteriorated materials [5].

To address these challenges, the use of vibrational spectroscopic techniques has been proposed in the literature, as it combines the well-known specificity towards molecular structures of such techniques and their consequent ability to identify different polymeric materials with the possibility of non-invasive analyses, particularly advantageous when investigating cultural heritage assets. For this reason, attenuated total reflection (ATR) and external reflection (ER) Fourier-transform infrared (FTIR) spectroscopy [4,6–8], as well as near-infrared (NIR) reflection spectroscopy [9], were used in particular in previous studies on cinematographic film supports.

Regarding the state of the art for the determination of the degree of substitution in cellulose acetate, traditional methods rely on titration, while nuclear magnetic resonance (NMR) has also been proposed as an alternative. However, both techniques require sampling and dissolution of the material [10]. The feasibility of using transmission FTIR spectroscopy has been demonstrated [10], showing a non-linear correlation between DS and the relative intensity of characteristic polymer peaks. A similar approach has been applied to films using non-invasive ATR-FTIR spectroscopy [4]. Furhermore, the shift of the first overtone band related to O-H stretching in the NIR spectra of cellulose acetate films has been correlated with their degree of substitution [11].

In the present work, the polymer supports of numerous cinematographic film samples of various brands and time periods—ranging from approximately 1895 to the first decade of the 21st century— were studied using a comprehensive approach based on vibrational spectroscopic techniques. Among the materials analyzed were Ozaphan films, which had never been studied before from the perspective of materials science. Introduced for the first time in the 1920s in France and subsequently adopted in Germany for small formats such as 16 mm, their production was interrupted during and immediately after World War II, but was then resumed until 1958. Their peculiarity lies in the absence of an emulsion layer, as the image was printed directly onto a cellophane support using the diazotype printing process [12].

The first objective of the work was to investigate the films using techniques that allow a completely non-invasive and, in principle, "in situ" analysis by means of portable instrumentation. This approach is especially valuable for the application in those contexts where films are preserved, such as archives and film libraries. For this reason, FTIR spectroscopy was applied in external reflection (ER) mode, not requiring any contact with the sample, both in the mid-infrared (MIR) range and in the longer-wavelength portion of the near-infrared (NIR) region. For the same reason, Raman spectroscopy was also used in this study, as its use has been reported in the literature for the characterization of cellulose-based heritage objects [13,14]. However, its application to motion picture films has so far been rather limited, with the exception of a study on the degradation of cellulose nitrate materials [15]. In particular, the Sequentially Shifted Excitation (SSE™) patented technology was used here to mitigate the issue of fluorescence emission, which is often associated with organic materials. This technology represents the up-to-date development of the so-called shifted excitation methods for extracting Raman information from an interfering background. These methods are based on the fact that, by varying the excitation laser wavelength during the acquisition of the Raman spectrum, a change

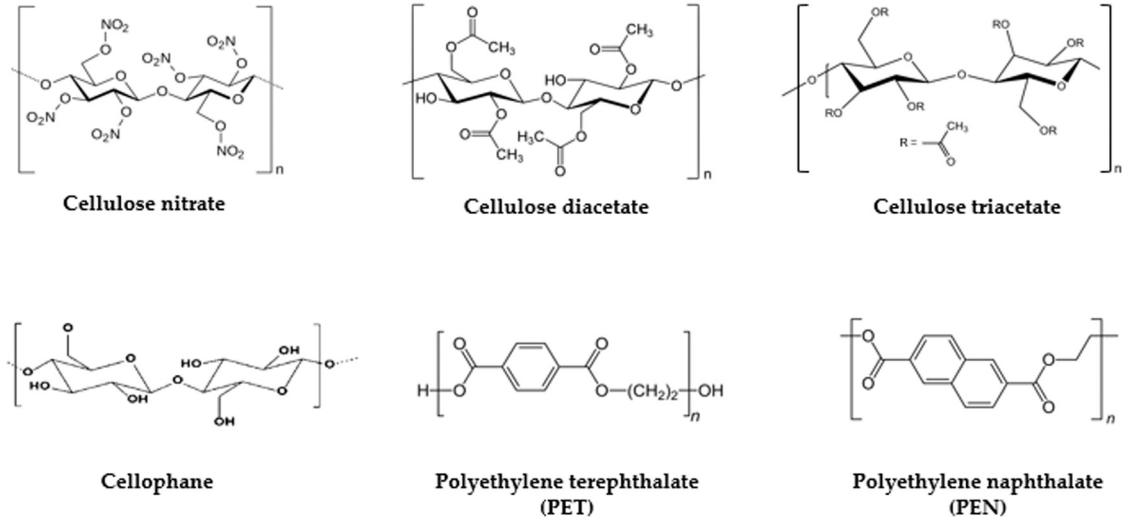

Fig. 1. Molecular structures of different polymers used as support in cinematographic films.

occurs in the position of the Raman bands in the spectral space, while unwanted spectral components such as those corresponding to fluorescence remain unchanged in the same space. In the simplest version, just two excitation wavelengths are used and the final Raman spectrum without the fluorescence contribution is obtained as the difference between the two measurements. In the SSE technology, diode lasers are used that operate at different temperatures and therefore deliver several slightly shifted wavelengths in the NIR region; a specific algorithm, which is part of the patent, allows the extraction of the spectral data in the Raman space [16].

The study, based on the significant number of film samples examined and on their representativeness in terms of different materials, made it possible to compare the aforementioned techniques from the point of view of the type of information they can provide. It is worth highlighting that the techniques considered differ first of all in the depth of penetration into the material. This depth is more limited and is around a few tens of micrometers for MIR radiation [17], while it is greater for NIR radiation, even reaching a few hundred micrometers [18]. This last fact applies to both ER-NIR measurements and Raman measurements with NIR excitation. Another important difference between the ER-MIR and ER-NIR techniques lies in the intensity of the absorptions observed in the two spectral regions. In fact, in the near infrared, overtone and combination vibrational bands are observed, with an intensity lower than the fundamental ones, and therefore the specular reflection spectra are less subject to distortions due to the combination of reflection and absorption contributions compared to those obtained in the mid-infrared region [19]. Finally, it is worth mentioning that IR and Raman spectroscopies are based on different selection rules, so they are usually complementary from the point of view of sensitivity towards different molecular structures [20].

Subsequently, in the second part of the work, using spectra from historical cellulose acetate films and reference standards acquired through diffuse reflection spectroscopy with benchtop instrumentation across the full NIR range (800–2500 nm, 12,500–400 cm^{-1}), a preliminary statistical model based on partial least squares (PLS) regression was developed to estimate the DS of film supports. The results obtained were then compared with those derived from ATR-FTIR spectra according to the procedure suggested in the literature [4].

2. Materials and methods

2.1. Motion picture film samples

The cinematographic film samples analyzed in this study, along with their main characteristics, are listed in Table 1. Most of these samples belong to the private collection of Dr. Valentina Rossetto, and selected examples are shown in Fig. 2. The more recent films, dated post-1950, were examined specifically in terms of the degree of substitution of cellulose acetate, the polymer constituting their support as determined previously in our laboratory. A comprehensive description of the cinematographic film samples is provided in Table S1 of the Supplementary Material.

The majority of the samples consisted of a limited number of frames and were in good chemical condition, though some exhibited mechanical damage such as tears or creases. Notable exceptions included two cellulose acetate films (DC2 and CINET), for which conservators diagnosed ongoing vinegar syndrome. Additionally, the Ozaphan films analyzed primarily displayed color alterations, with the presence of orange, brown, or purple spots.

2.2. Reference materials

To evaluate the degree of substitution (DS) of cellulose acetate films, reference materials and mixtures with known DS values, listed in Table 2, were used.

α-Cellulose and Eastman cellulose acetate (DS = 2.4) were kindly

Table 1
Film samples with different polymer bases analysed in the present work. Legend: B/W = black and white.

Sample	State of conservation	Description	Film support identified in the present work
gr1_1A	Good	35 mm Color: stencil (*pochoir*) Probably dated between 1907–1908	Cellulose nitrate
gr1_1B	Good	35 mm Color: B/W 1896 – 1899	Cellulose nitrate
gr1_2A	Quite good	35 mm Color: orange/yellow tinting Probably Pathè brand and post 1909	Cellulose nitrate
gr1_2B	Possible degradation of the emulsion layer	35 mm Color: yellow tinting but bleached Post 1909	Cellulose nitrate
gr1_2C	Good Vertical tear in a frame	35 mm Color: yellow tinting Post 1909	Cellulose nitrate
gr1_3	Good	35 mm Color: yellow tinting very bleached. Film manufacture "Società Anonima Ambrosio Torino". Probably between 1907 and 1909.	Cellulose nitrate
gr1_4	Good	35 mm Color: blue/green toning Late 1910s to early 1920s	Cellulose nitrate
gr1_5	Good	35 mm Color: B/W Post 1930	Cellulose nitrate
gr1_6A	Good	35 mm Color: chromogenic film Probably Kodak, year 2008	Polyethylene terephthalate (PET)
gr1_6B	Medium	35 mm Color: B/W Pathè film, probably between 1911–1914	Cellulose acetate
gr1_6pers	Very good	Color: chromogenic film Early 2000s	Polyethylene terephthalate (PET)
gr1_6top	Very good	35 mm Color: B/W 1940s	Cellulose nitrate
gr2_1	Very good	16 mm Color: B/W 1950s	Cellulose acetate
gr2_2	Very good	16 mm Color: B/W The writing "Safety" on the edge identifies its support as an acetate. Post 1950.	Cellulose acetate
gr2_3	Mechanically damaged	9.5 mm Color: B/W The writing "Gevaert Safety AB" on the edges suggests cellulose acetate butyrate [21]. 1935–1950	Cellulose acetate
gr2_4	Partly covered with adhesive tape	28 mm Color: B/W Pathè-KOK 1912–1929	Cellulose acetate
gr2_5A	Very good	35 mm Color: red tinting Film *La bocca suggellata*	Cellulose nitrate

(*continued on next page*)

Table 1 (*continued*)

Sample	State of conservation	Description	Film support identified in the present work
		(1921), by Tornielli Film (Torino).	
gr2_5B	Very good	35 mm Color: red tinting Tiziano company production (Torino). 1920 - 1921	Cellulose nitrate
gr2_6A	Projection stripes Vertical tear in a frame	28 mm Color: B/W Pathè-KOK 1912–1929	Cellulose acetate
EAST	Quite good	35 mm Color: chromogenic film Eastman Kodak 1990, confirmed by the edge codes Δ+ Δ.	Cellulose acetate
RAOUL1 RAOUL2	Good	35 mm Color: chromogenic film Eastman Kodak The code 5296 on the edge indicates a polyester film. Probably 1993	Cellulose acetate
DUMBO	Good	8 mm Color: B/W Post 1950	Cellulose acetate
DC2	Stiffened sample ("vinegar syndrome" ongoing?)	16 mm Color: B/W Post 1950	Cellulose acetate
CINET	"Vinegar syndrome" underway	16 mm Color: B/W Post 1951	Cellulose acetate
CR		Unknown film and year	Cellophane
A8	Reddish brown stain Crystalline efflorescences	16 mm From film *Schneewittchen* 1930	Cellophane
A13	Orange/brown stains	16 mm From film *Überfall auf den Goldexpress* 1950s	Cellophane
A14a	Dried liquid residue (probably projector oil)	16 mm From Monatsschau 9/39 (monthly newsree) September 1939	Cellophane
A14b	Purple stain on the side of the frame	Unknown film and year	Cellophane
A15	Orange halos	16 mm? Unknown film and year Film previously treated with acid	Cellophane
A17		Probably monthly news 1939	Cellophane

provided by Gibaplast (Varese, Italy), while cellulose triacetate (DS = 3) was supplied by Cayman Chemical. A cellulose acetate sample with DS = 2 was kindly donated by Dr. Marco Ortenzi. The DS value is related to the weight percentage of acetyl groups (%A) according to the following equation:

$$DS = 162 \times \%A / (4305 - 43 \times \%A)$$

Samples with specific DS values were prepared by mixing appropriate amounts of α-cellulose powder (%A = 0) and cellulose acetate powder (2.4AC or 2AC) (%A = 39.8 or 34.7), as detailed in Table 2.

To ensure comparability with cinematographic film samples, transparent films were produced by dissolving the polymer powders in acetone (10 % m/m) and cellulose triacetate in pure chloroform. The solutions were kept under magnetic stirring until they reached a viscous consistency. Finally, the solutions were spread onto glass slides, forming transparent films upon drying.

2.3. Instrumental methods

2.3.1. ER-FTIR spectroscopy

For non-invasive, contactless analyses in reflection mode, a Bruker Alpha FTIR spectrophotometer equipped with a reflection module was used. The instrument features a deuterated triglycine sulfate (DTGS) detector, which operates at room temperature and provides a linear response within the spectral range of 7500–375 cm^{-1} . The FTIR spectrophotometer collects spectra from a sample area with a diameter of approximately 6 mm at a resolution of 4 cm^{-1} . An integrated camera allows the operator to precisely select the measurement area.

FTIR spectra were acquired as the sum of 200 scans, following the acquisition of a background spectrum on a gold mirror. Each sample was positioned 1.5 cm from the instrument. Reflection spectra in the MIR region were processed using the Kramers–Kronig transform in the Bruker OPUS software, while those in the NIR range were converted into pseudo-absorbance values using Log(1/R).

2.3.2. ATR-FTIR spectroscopy

Attenuated total reflection (ATR) FTIR spectra were acquired using a Jasco FTIR-470 spectrometer equipped with an ATR accessory featuring a single-reflection ZnSe crystal at a 45° angle of incidence. Each spectrum was obtained by summing 256 accumulations over the spectral range of 4000–700 cm^{-1} , with a resolution of 4 cm^{-1} . The contributions of CO_2 and water vapor were compensated by subtracting a baseline spectrum.

2.3.3. Raman spectroscopy

Raman measurements on the films were conducted using a Bruker BRAVO handheld spectrometer. The instrument employs patented SSE™ technology, which minimizes interference from fluorescence emission. Spectra were excited using two diode lasers operating at different temperatures, emitting at 785 nm and 852 nm, respectively. The spectral data were collected in two ranges, 2000–3200 cm^{-1} and 300–2000 cm^{-1} , with a dedicated algorithm extracting the final Raman spectra.

The instrument provides an average spectral resolution of approximately 11 cm^{-1} , with laser power always kept below 100 mW for both lasers. Acquisition time and the number of accumulations were automatically set by the instrument. To prevent potential damage from laser-induced heating, film samples suspected of having cellulose nitrate support were excluded from this analysis due to the lower thermal stability of this polymer compared to other cellulose esters [22].

2.3.4. Diffuse reflection NIR spectroscopy

This analysis was performed exclusively on cellulose acetate-supported films and reference materials using a Jasco UV/VIS/NIR V-570 spectrometer equipped with an integrating sphere internally coated with $BaSO_4$. Spectra were collected over the range of 800–2500 nm (12,500–4000 cm^{-1}) at an acquisition rate of 200 nm/min and a resolution of 20 nm. A Mylar® polyester target with an assumed reflectance of 100 % was used as the reference.

2.4. Mathematical methods

2.4.1. PLS regression

The diffuse reflectance spectra acquired in the NIR region for the cellulose acetate-based reference materials (Table 2) were used to construct a model using Partial Least Squares (PLS) regression. This model enabled the estimation of the acetyl content percentage and, consequently, the degree of substitution (DS) of the examined cinematographic films with the same base polymer. The statistical analysis was performed using Minitab version 13. The software provided the

Fig. 2. Some examples of film samples with different chronologies analysed in this work.

Table 2
Reference materials used to determine the DS values of the cinematographic films.

Standard film	% Acetylation	DS
Cellulose	0	0
Mixture 1 (0.03 g α-cellulose + 0.03 g 2AC)	17.7	2
Mixture 2 (0.03 g α-cellulose + 0.028 g 2.4AC)	19.3	0.9
Mixture 3 (0.05 g α-cellulose + 0.128 g 2.4AC)	28.5	1.5
Mixture 4 (0.05 g α-cellulose + 0.33 g 2.4AC)	34.7	2
2.4AC	39.8	2.4
3AC	44.4	3

values of R^2, i.e. the percentage of total variation in the response that is explained by predictors in the model, and predicted R^2, which indicates how well the model predicts responses for new observations. The latter value was determined by cross-validation of the model with the leave-one-out method, that calculates potential models leaving out one observation at a time. The formula used were:

$$R^2 = 1 - \frac{SS\ Error}{SS\ Total}$$

where $SS\ Error = \sum_{i=1}^{n} (y_i - \hat{y}_i)^2$, with y_i observed response and $\hat{y}_i$fitted response for the i-th observation and $SS\ Total = \sum_{i=1}^{n} (y_i - \bar{y}_i)^2$, with $\bar{y}_i$ mean response for the i-th observation, and

$$Predicted\ R^2 = 1 - \frac{PRESS}{SS\ Total}$$

where $PRESS = \sum_{i=1}^{n} (y_i - \hat{y}_{(i)})^2$, with $\hat{y}_{(i)}$fitted response for the omitted observation when using the leave-one-out method.

Prior to applying the regression analysis, the NIR spectra were truncated to the range of 1000–2500 nm (10,000–4000 cm^{-1}) using Grams AI software (Thermo Fisher Scientific). To minimize baseline slope variations, the second derivatives of the spectra were calculated using the gap algorithm (gap width: 20 nm). The gap derivative algorithm approximates the analytical derivative by determining the difference between two spectral points separated by a given distance, which is the gap width.

2.4.2. Calibration function from ATR-FTIR spectra

As mentioned previously, a quantitative relationship expressed by a second-order polynomial between FTIR spectral data, i.e. absorbance values and/or areas of specific peaks, and the DS of cellulose acetate polymers has been reported in the literature [10]. Thus, the use of ATR-FTIR spectra to non-invasively estimate the DS values for cellulose acetate films is now a recognized procedure [4,11]. For this reason, in the present study the reported correlation was used to verify the DS values obtained from the PLS regression of NIR spectra (see Section 2.4.1).

After baseline correction of the ATR spectra of reference materials, performed using the Grams AI software, the ratio of the areas of bands at 1214 cm^{-1} (C–O stretching of acetyl groups) and 1030 cm^{-1} (C–O–C stretching in the anhydroglucose unit backbone) was calculated. This ratio was then correlated with the DS value using a second-order polynomial function, implemented in Microsoft Excel.

3. Results and discussion

3.1. Identification of the polymer film base: a comparison of the techniques

3.1.1. ER-FT-MIR spectroscopy

ER-FT-MIR spectroscopy, which unlike the ATR-FTIR technique allows analysis without any direct contact with the sample, first of all makes it possible to separately characterize the polymer support and the emulsion layer of the films, thanks to the above-discussed limited penetration depth of the technique. Fig. 3 presents the IR spectra obtained from the emulsion side of films with different types of polymer support. In all cases, the characteristic amide bond signals were identified at 1636 cm^{-1} (C═O stretching) and 1540 cm^{-1} (N–H bending and C–N stretching), together with a band at 1440 cm^{-1} corresponding to CH_2 deformation. These characteristics are consistent with gelatin [23], the primary protein-based component of the emulsion layer in motion picture films. The Ozaphan films were excluded from this comparison, as they lack an emulsion layer, as explained in the Introduction.

Notably, in spectrum (a) of Fig. 3, due to a film with a cellulose nitrate support, a band at 840 cm^{-1} is observed. This peak is not attributed to the emulsion layer but instead to the underlying cellulose nitrate support (as discussed below). The reason why only this band of the polymer is observed when the film is examined from the emulsion side is that it is the only one located in a range where the overlying gelatin layer has no relevant absorptions and is therefore relatively transparent to the

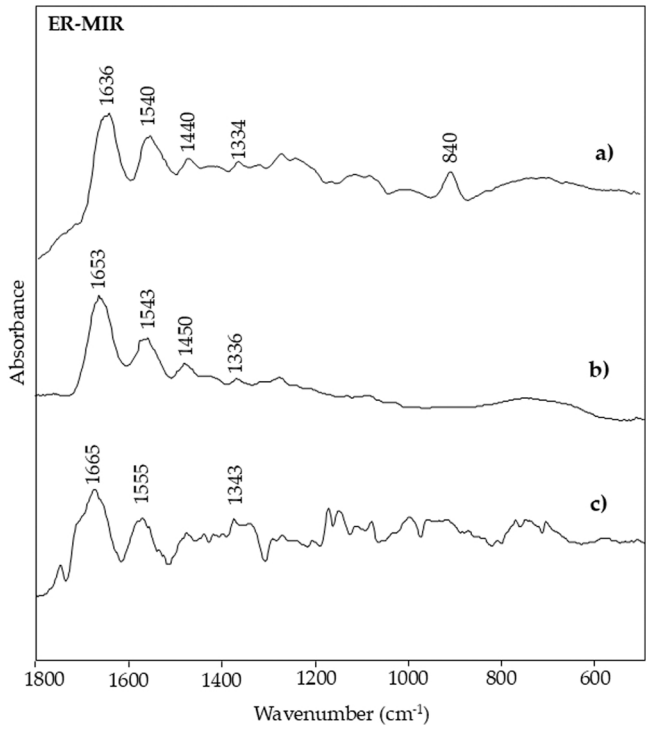

Fig. 3. FTIR spectra of the emulsion layer of film samples with different polymeric support: (a) gr1_2A (cellulose nitrate), (b) gr2_1 (cellulose acetate), (c) gr1_6pers (PET).

radiation.

When the films were examined from the polymer side, characteristic spectra were obtained as expected for the different supports. An example for each support is shown in Fig. 4 (box I), while the spectra acquired for all the films examined are reported in Figs. S1–S4 (Supplementary Material).

In particular, cellulose nitrate supported films, corresponding to eleven of the analyzed samples, provided characteristic IR bands at approximately 1651, 1281, and 846 cm^{-1} for the vibrational modes of the nitrate group (NO_2 asymmetric and symmetric stretching and N–O stretching) [7] (Fig. 4(a), box I). The bands around 1119, 1070, and 1004 cm^{-1} are instead attributed to the stretching motion of the C–O–C bond in cellulose [13].

For cellulose acetate supported films, corresponding to six of the samples analyzed, the ER-MIR spectra (Fig. 4(b), box I) are dominated by the characteristic bands of the acetyl group at 1750, 1370, and 1233 cm^{-1} [9], while the band at 1050 cm^{-1} corresponds to the C–O–C stretching of the cellulose bond.

An interesting case, demonstrating if necessary the excellent performance of FTIR spectroscopy for the characterization of films with cellulose-derived polymer supports, is represented by sample gr2_3, i.e. the piece of film labeled “Gevaert Safety AB” on the edge (see the image in Table S1, Supplementary Material). This code has historically been used by the manufacturer to indicate an acetate butyrate support [21, 24], but the ER-MIR spectrum corresponds to a cellulose acetate base, as demonstrated by comparison with the reference spectrum of an acetate butyrate polymer (Fig. S5, Supplementary Material). The spectrum of acetate butyrate is characterized by a distinct pattern, in particular a band around 1170 cm^{-1} attributed to the C–O–C stretching mode [25]. The relative intensity of this band, compared to that at approximately 1230 cm^{-1}, increases with a greater percentage of butyrate [26]. Sample gr2_3, therefore, represents an example of a misleading code. Most likely this is a positive image printed on cellulose acetate film, derived from a cellulose acetate butyrate negative. The code from the original negative persists in the print, a not uncommon occurrence [5].

Unlike the samples discussed above, the spectra obtained for the two films with a PET support (an example is shown in Fig. 4(c), box I) show a

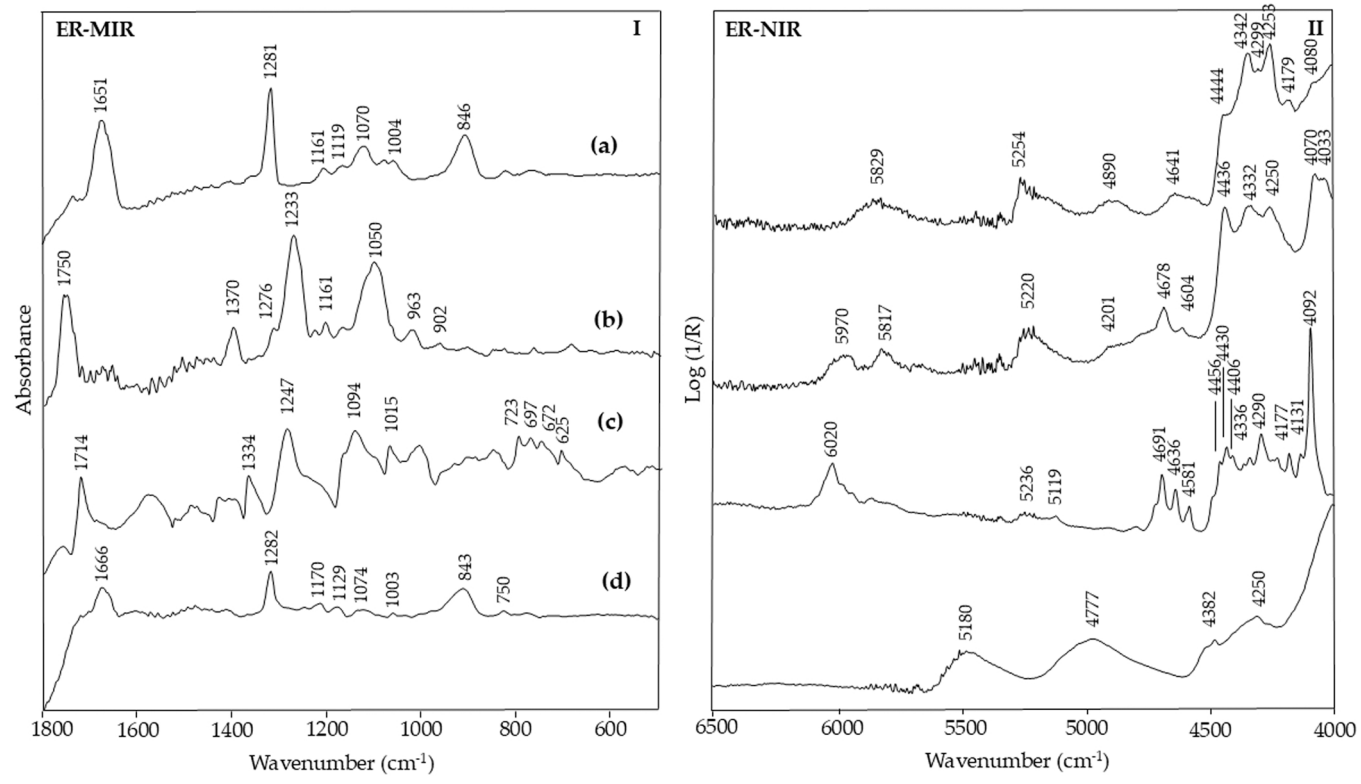

Fig. 4. ER-FTIR spectra in the MIR (box I) and NIR ranges (box II) of motion picture film samples with different polymeric support: (a) gr1_3 (cellulose nitrate), (b) gr2_2 (cellulose acetate), (c) gr1_6A (PET) and (d) A8 (cellophane with nitrocellulose coating).

rather distorted, derivative-like pattern, probably due to the combination of specular and diffuse reflectance from the polymer surface, which is a possible drawback of external reflection spectra in the mid-IR range as explained in the Introduction. This may be due to a perhaps less smooth surface of the PET film compared to those derived from cellulose, when used as a base for motion picture films [27]. Nevertheless, some of the characteristic bands of PET can still be recognized, particularly at 1714, 1334, 1247, 1094, 1015, and 723 cm^{-1}, which correspond to those reported in the literature for this polymer [28,29].

Another characteristic aspect of ER-MIR measurements, namely the limited penetration depth of the radiation into the sample, is evident in the case of the spectra obtained for the Ozaphan films (Fig. 4(d), box I). As mentioned in the Introduction, these films have a cellophane base, consisting of cellulose regenerated by treatment with alkali and carbon disulfide [30]. However, the observed spectral pattern closely resembles that of cellulose nitrate (Fig. 4(a)). This is due to the fact that in Ozaphan films a thin nitrocellulose coating was typically applied to the cellophane layer as a water- and moisture-resistant lacquer [31]. The limited depth of penetration of the mid-infrared radiation allows observation only of the bands of the surface coating and not of those corresponding to the cellophane.

3.1.2. ER-FT-NIR spectroscopy

The different support materials of the examined films also exhibit very characteristic spectra in the NIR region (6500 to 4000 cm^{-1}, Fig. 4, box II), which allow for easy distinction between them. Significant bands in the 4500–4000 cm^{-1} range, which had not been reported in previous studies on motion picture films, were also observed in this investigation. For cellulose acetate and nitrate, these bands can be tentatively assigned to the combination of vibrational modes of the cellulose backbone, specifically C–H stretching and C–C stretching (around 4060 and 4020 cm^{-1}), C–H stretching and CH_2 deformation (around 4250 cm^{-1}), C–H stretching and O–H stretching (around 4330 cm^{-1}), and O–H stretching and C–O stretching (around 4430 cm^{-1}). Furthermore, a band at about 5220 cm^{-1} is observed, which is attributed to the combination of O–H stretching and deformation of absorbed water molecules [32]. The NIR spectra of the cellulose acetate supports are also characterized by a signal at 4680 cm^{-1}, which is associated with the acetylation of cellulose and attributed to the combination of C–H stretching and C═O stretching of acetyl groups [33]. For cellulose nitrate, two broad signals at around 4890 and 4640 cm^{-1} are observed, which have been previously assigned to the combination of vibrational modes of O–H groups. These are still present in cellulose nitrate, as it does not usually undergo complete substitution of hydroxyl groups with nitrate groups [34].

However, it is in the case of PET-based films that one of the advantages deriving from the use of external reflection of NIR radiation becomes evident. Indeed, as can be deduced from Fig. 4(c), in ER-FTIR this polymeric support is recognized more clearly by its NIR spectrum than by its MIR spectrum, as it does not show any distortion of the bands thanks to the lower extinction coefficients in this spectral region (see Introduction). The NIR spectrum of PET is characterized by a sharp band at 4092 cm^{-1}, typically due to the presence of the aromatic ring in the polymer structure [35], which is also responsible for the three bands at 4691, 4636, and 4581 cm^{-1}.

Finally, another property related to NIR radiation compared to MIR radiation and already mentioned above, i.e. its greater depth of penetration, is demonstrated by the NIR reflection spectra of the Ozaphan films (Fig. 4(d), box II), which correctly show the typical pattern expected for a cellulosic material such as cellophane [32], while the bands in the MIR spectrum were due to the cellulose nitrate surface coating (see Section 3.1.1).

3.1.3. Raman spectroscopy

Raman spectroscopy with SSE™ technology was only applied for cellulose acetate, PET and Ozaphan films, to avoid thermal degradation in the case of cellulose nitrate as mentioned above. Examples of the spectra obtained for each material are shown in Fig. 5 and the spectra acquired for all films examined are reported in Figs. S6–S8 (Supplementary Material).

For films with the first two base materials, cellulose acetate and PET, the Raman spectra confirmed the assignments made on the basis of FTIR spectra. However, for the cellulose acetate supports the strongest signal in the spectra (Fig. 5(a)), located at 1006 cm^{-1}, is not due to the polymer, but to triphenyl phosphate (TPP), one of the typical plasticizers of acetate plastics [36] to which also the peak at 717 cm^{-1} is assigned. The support of the cellulose acetate films is identified by Raman peaks due to the cellulose backbone at 1459 cm^{-1} (CH_2 deformation), 1380 cm^{-1} (deformation of CH bonds) and 1157 cm^{-1} (C-O and C-C stretching) and to the vibrations of the acetyl groups at 1745 cm^{-1} (C═O stretching), 1072, 910 and 655 cm^{-1} [37,38]. The prevalence of the 1006-cm^{-1} band, assigned to the symmetric stretching of the aromatic ring of TPP [39], can be related to the significant change in polarizability associated with C═C stretching vibrational modes [20] and to the resulting higher intensity of the corresponding Raman band.

For PET films Raman spectra with a better signal-to-noise ratio could be obtained (Fig. 5(b)), again probably thanks to the aromatic rings present in the structure of the PET molecule. The Raman spectra of these film show the characteristic peaks at 1727 cm^{-1} (C═O stretching), 1613 cm^{-1} (ring mode 8a in Wilson's notation), 1455 cm^{-1} (CH_2 bending and OCH bending), 1290 cm^{-1} (C(O)–O stretching) and 1186 cm^{-1} (ring in-plane deformation of C–H bonds and C–C stretching) [40].

Finally, the prevalence of the signals due to vibrations of molecular structures with greater variations in polarizability can also explain why the Raman spectra of most Ozaphan films show peaks at 1574, 1444 and 1370 cm^{-1} (Fig. 5(c)) which cannot be attributed to the cellophane support [41] but are most probably related to the azo dye formed in printing the image on the cellophane itself [42]. The observed bands can be assigned respectively to a ring stretching mode, to the N = N bond stretching and to C═N and C-C stretching modes [43]. An example of the molecular structure of such dyes is shown as well in Fig. 5(c). Only in the case of the piece of film A15, without an image (see Table S1, Supplementary Material), could the Raman spectrum characteristic of cellophane be obtained, with bands at 1462, 1374, 1314, 1260, 1116, 1094 and 900 cm^{-1} [41]. A remnant of the strongest band of the support at around 1090 cm^{-1} can however be observed also in the Raman spectra of films for which the contribution of the dye is predominant (Fig. S8, Supplementary Material). Interestingly, in any case, the surface coating formed by cellulose nitrate, detected by ER-MIR spectroscopy, was not observed by Raman spectroscopy, similarly to ER-NIR measurements, due to the greater penetration depth of near-infrared radiation.

3.2. Estimation of DS for the support of cellulose acetate films

The stability of cellulose acetate supports largely depends on a high degree of substitution of their -OH groups. However, in the case of motion picture film, achieving this required a highly complex manufacturing process, including the pre-conditioning of the cellulose. As a result, various types of acetate with differing levels of substitution were used during the early period of cinema, typically ranging from 1.5 to 2.3. This relatively low degree of substitution has contributed to their instability and brittleness. In 1948, when Eastman Kodak introduced cellulose triacetate for 35 mm films, the substitution rate still remained below 2.76 due to the spatial constraints of the acetyl groups within the polymer chain [3,21].

To estimate the DS values for the examined films with a cellulose acetate support, a PLS model was constructed based on NIR spectra acquired in the range 1000 - 2500 nm (10,000 - 4000 cm^{-1}) using the diffuse reflection technique, with a benchtop spectrometer equipped with an integrating sphere (see Sections 2.3.4 and 2.4.1). This method

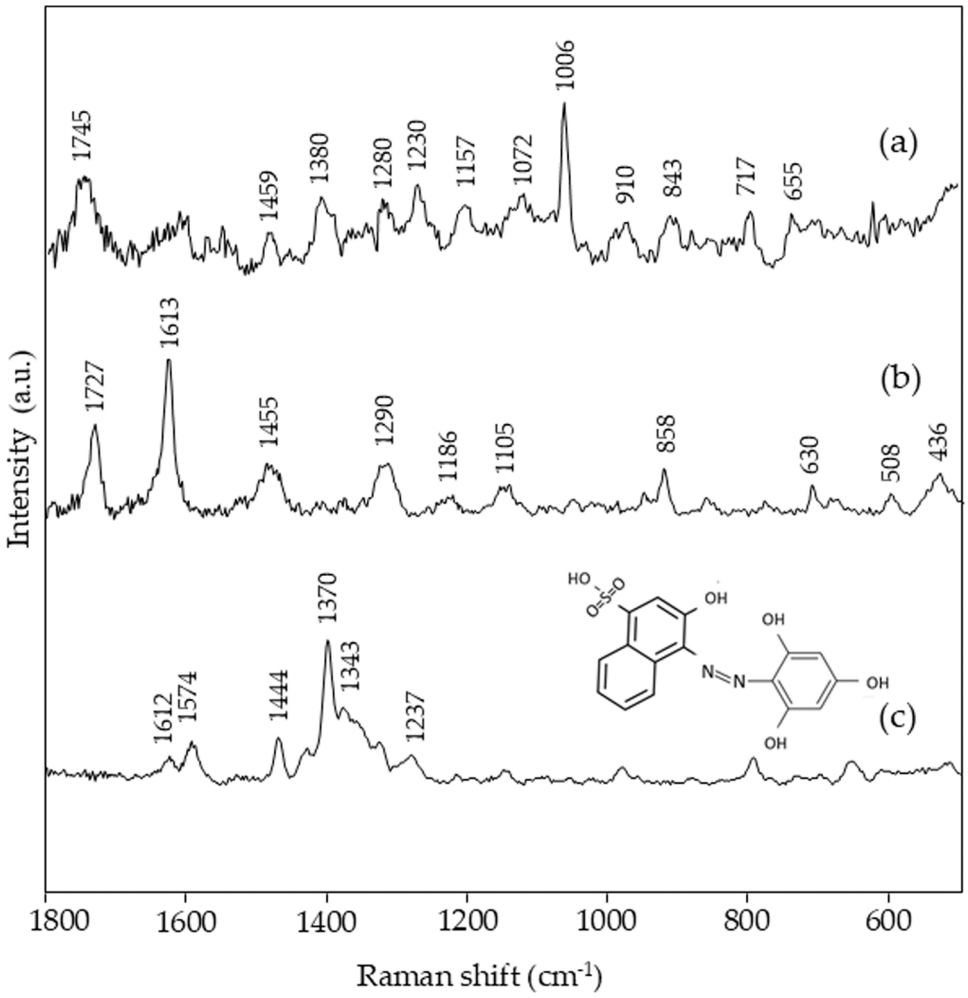

Fig. 5. SSE™ Raman spectra of motion picture film samples with different polymeric support: (a) gr2_4 (cellulose acetate), (b) gr1_6pers (PET), (c) A8 (Ozaphan film).

allowed us to investigate a broader spectral range and obtain a better signal-to-noise ratio, compared to the portable instrumentation, thus providing a more efficient quantitative evaluation. Consequently, additional bands were observed, compared to those already reported in Section 3.1, at approximately 8600 cm^{-1} (2nd overtone of CH_3 stretching) with a shoulder at 8280 cm^{-1} (2nd overtone of CH_2 stretching), 7020 cm^{-1} (1st overtone of OH stretching, amorphous region) with a shoulder at 7415 cm^{-1} (combination of 1st overtone of C-H stretching and C-H bending), and 5990 and 5830 cm^{-1} (1st overtone of C-H stretching) (see Figs. S12 and S13, Supplementary Material) [33].

For the PLS model developed based on the spectra of the reference materials listed in Table 2 an R^2 value of 0.998 and a predicted R^2 value of 0.812 were obtained for three components, as explained in Section 2.4.1. According to reference [44] the predicted R^2 value obtained for our model, being higher than 0.67, corresponds to a high predictive accuracy.

The model was then used to estimate the DS value for the six film samples with a cellulose acetate base examined in the present study and, additionally, for six more pieces of cellulose acetate films dated after 1950 (Table 1), to evaluate the evolution of the material over time as a base for motion picture films. The results are listed in Table 3. As explained in Section 2.4.2, the DS values obtained from the PLS model based on NIR spectra were compared with those calculated from the calibration curve derived from ATR-FTIR spectra of reference materials (Figs. S10 and S11, Supplementary Material) as described in Section 2.4.2 and having an R^2 value of 0.926. In general, the percentage deviation of the DS values between the ATR and PLS models is less than 10 %, confirming the validity of the proposed method.

Table 3
Comparison between DS values estimated from ATR spectra and with the PLS model based on NIR spectra. Legend: Δ % = percentage difference between the values obtained for each sample with the two methods.

Degree of Substitution (DS)			
sample	**ATR**	**PLS model**	**Δ %**
1950 – 1993 films			
CINET	2.03	2.16	6.52
DC2	2.55	2.47	3.08
DUMBO	2.40	2.25	6.42
EAST	2.38	2.50	4.85
RAOUL1	2.47	2.39	3.33
RAOUL2	2.47	2.29	7.75
1911 – 1950 films			
gr1_6B	1.46	1.55	6.34
gr2_1	1.85	1.88	1.70
gr2_2	1.93	1.91	0.71
gr2_3	1.14	1.19	4.47
gr2_4	1.28	1.21	5.71
gr2_6A	1.52	1.46	3.95

The more recent films (first group in Table 3) have a higher DS than the films dated before 1950 (second group in Table 3), as expected considering the evolution of the material and/or the better preservation of the films. In fact, in 1951, cellulose triacetate became the standard for

all Eastman Kodak films [3]. Consequently, films from the 1950s probably originally had a cellulose triacetate base (maximum DS = 2.76), but lower DS values are currently observed due to partial degradation. In fact, some of these films (DUMBO and DC2) show signs of ongoing "vinegar syndrome". CINET (16 mm), DC2 (16 mm), and DUMBO (8 mm) are the so-called Kodak small formats introduced in the 1920s on cellulose diacetate support and still produced today [45,46]. The DS calculated by the PLS-based model, however, is higher than 2, which is consistent with the dating of the films and the fact that, from 1951, cellulose triacetate became the standard support also for Eastman Kodak amateur roll films [47]. Therefore, it is likely that these films have a cellulose triacetate base that has degraded over time.

In contrast, the support of the films of the second group appears to be cellulose diacetate. Consistently, samples gr2_4 and gr2_6A are pieces of 28 mm Pathé-KOK films dated around 1910, when this format was officially introduced on the market with cellulose diacetate support. In particular, samples gr2_3 and gr2_4 have a DS of less than 1.5 and, although appearing in good condition, are probably undergoing deterioration. It is interesting to note that the method also gave a reliable result for the sample gr2_3, formed almost entirely by a dark image, for which therefore for example the position of the band around 7000 cm^{-1}, previously proposed in the literature as a criterion to estimate the DS value [11], cannot be determined exactly.

4. Conclusions

The present study confirms the effectiveness of vibrational spectroscopy, applied using portable instrumentation, for the non-invasive identification of polymer bases in motion picture films. The use of portable spectrometers makes the techniques suitable for analyses conducted directly where the films are stored, such as in archives and film libraries. Moreover, the spectroscopic approach has proven effective not only for the most common types of support but also for unusual ones, such as Ozaphan films.

ER-FTIR spectroscopy in the MIR region is particularly suitable for identifying polymer supports based on cellulose, such as cellulose acetate and nitrate, due to the characteristic functional groups. Regenerated cellulose, such as cellophane, can also be recognized; however, if a protective layer is present, as in the Ozaphan films, only the latter will be detected in the MIR range. Conversely, the synthetic polymer base PET usually exhibits significantly distorted bands in this spectral region. In contrast, in the NIR region, even limited to its longer-wavelength portion, characteristic spectra are obtained for all supports, even in the presence of a surface coating and without band distortion, thanks to the weaker absorptions typically observed in this spectral range.

Raman spectroscopy is less efficient when cellulose derivatives are involved, as they are rather weak scatterers and thus tend to suffer from fluorescence background interference, even when a dedicated technology is employed, as in the present work. On the other hand, good quality spectra are usually obtained for PET films. Furthermore, the Raman technique enables the identification of additional film components, for example plasticizers such as triphenyl phosphate in cellulose acetate films and azo dyes in Ozaphan films. The rather strong Raman bands associated with molecular structures containing aromatic rings can explain the above observations.

Finally, NIR spectroscopy also proved useful for evaluating the DS value of cellulose acetate films, a parameter linked to the chronology and conservation state of the film. In this case, a benchtop spectrometer was used to access a wider spectral range than portable instrumentation and a method based on a preliminary model constructed via PLS regression was proposed. Good results were obtained even when only portions of films with dark images were available, where broad absorption extending from the visible to the near-infrared region overlaps combination and overtone vibrational bands. This method paves the way for the development of future refined models and further studies on other types of film bases.

CRediT authorship contribution statement

Alessia Buttarelli: Writing – original draft, Visualization, Investigation, Formal analysis, Data curation. **Margherita Longoni:** Writing – review & editing, Supervision, Investigation. **Valentina Rossetto:** Writing – review & editing, Resources, Data curation, Conceptualization. **Silvia Bruni:** Writing – review & editing, Supervision, Resources, Methodology, Formal analysis, Data curation, Conceptualization.

Declaration of Competing Interest

The authors declare that they have no known competing financial interests or personal relationships that could have appeared to influence the work reported in this paper.

Appendix A. Supporting information

Supplementary data associated with this article can be found in the online version at doi:10.1016/j.vibspec.2025.103818.

Data availability

The data are available in the paper

References

[1] Eastman Kodak Company, Film structure, in: The essential reference guide for filmmakers, Eastman Kodak Company, Publisher, Rochester, 2007, pp. 29–32.
[2] C. Montanaro, Dall'argento al pixel. Storia della tecnica del cinema, first ed., Linea Edizioni, Padova, 2019.
[3] History, Science and Storage of Cellulose Acetate Film Base, ⟨https://cool.culturalheritage.org/videopreservation/library/history_science_storage_of_acetate_base_film_16b.pdf⟩, 2009 (accessed 31 January 2025).
[4] S. Nunes, F. Ramacciotti, A. Neves, E.M. Angelin, A.N. Ramos, É. Roldão, N. Wallaszkovits, A.A. Armijo, M.J. Melo, A diagnostic tool for assessing the conservation condition of cellulose nitrate and acetate in heritage collections: quantifying the degree of substitution by infrared spectroscopy, Herit. Sci. 8 (2020) 1–14, https://doi.org/10.1186/s40494-020-00373-4.
[5] NEDDC Northeast Document Conservation Center, A Short-guide to Film-base Photographic Materials Identification. ⟨https://www.nedcc.org/free-resources/preservation-leaflets/5.-photographs/5.1-a-short-guide-to-film-base-photographic-materials-identification,-care,-and-duplication⟩, 2023 (Accessed 31 January 2025).
[6] E.A. Carter, B. Swarbrick, T.N. Harrison, L. Ronai, Rapid identification of cellulose nitrate and cellulose acetate film in historic photograph collections, Herit. Sci. 8 (2020) 1–13, https://doi.org/10.1186/s40494-020-00395-y.
[7] D. Estupiñán Méndez, T. Allscher, Advantages of external reflection and transflection over ATR in the rapid material characterization of negatives and films via FTIR spectroscopy, Polymers 14 (2022) 808, https://doi.org/10.3390/polym14040808.
[8] S. Noohi, H. Asadian, Application of FTIR microscopy to identify some glass plates of Golestan palace photo archive, Ir. Cons. Sci. J. 1 (2017) 48–53.
[9] E. Catelli, G. Sciutto, S. Prati, M.V.C. Lozano, L. Gatti, F. Lugli, S. Silvestrini, S. Benazzi, E. Genorini, R. Mazzeo, A new miniaturised short-wave infrared (SWIR) spectrometer for on-site cultural heritage investigations, Talanta 218 (2020) (2020) 121112, https://doi.org/10.1016/j.talanta.2020.121112.
[10] P. Fei, L. Liao, B. Cheng, J. Song, Quantitative analysis of cellulose acetate with a high degree of substitution by FTIR and its application, Anal. Methods 9 (2017) 6194–6201, https://doi.org/10.1039/c7ay02165h.
[11] M.V. Chavez Lozano, E. Catelli, G. Sciutto, S. Prati, E. Genorini, R. Mazzeo, A non-invasive diagnostic tool for cellulose acetate films using a portable miniaturized near infrared spectrometer, Talanta 255 (2023) 124223, https://doi.org/10.1016/j.talanta.2022.124223.
[12] C. Thielemann, L. Armellin, B. Sarti, A. Plutino, Ozaphan films: preliminary study on color analysis and digitization, Res. Cult. Sci. Books. (2023) 249–256.
[13] C. Paris, C. Coupry, Fourier transform Raman spectroscopic study of the first cellulose-based artificial materials in heritage, J. Raman Spectrosc. 36 (2005) 77–82, https://doi.org/10.1002/jrs.1288.
[14] O. Madden, K.C. Cobb, A.M. Spencer, Raman spectroscopic characterization of laminated glass and transparent sheet plastics to amplify a history of early aviation 'glass, J. Raman Spectrosc. 45 (2014) 1215–1224, https://doi.org/10.1002/jrs.4618.
[15] A. Neves, E.M. Angelin, É. Roldão, J. Melo, New insights into the degradation mechanism of cellulose nitrate in cinematographic films by Raman microscopy, J. Raman Spectrosc. 50 (2019) 202–212, https://doi.org/10.1002/jrs.5464.
[16] C. Conti, A. Botteon, M. Bertasa, C. Colombo, M. Realini, D. Sali, Portable sequentially shifted excitation Raman spectroscopy as an innovative tool for in situ

chemical interrogation of painted surfaces, Analyst 141 (2016) (2016) 4599–4607, https://doi.org/doi: 10.1039/c6an00753h.
[17] Y. Le Maoult, F. Schmidt, Infrared radiation applied to polymer processes, in: N. Boyard (Ed.), Heat Transfer in Polymer Composite Materials: Forming Processes, Wiley, London, UK, 2016, pp. 385–423, https://doi.org/10.1002/9781119116288.ch13.
[18] W.G. Haanstra, W. Hansen, M.J.G. Huys, Information depth of Vis-NIR light in polyethylene films using transmission and reflectance measurements, Appl. Spectrosc. 52 (1998) 863–868, https://doi.org/10.1366/0003702981944409.
[19] G.F. Monnier, A review of infrared spectroscopy in microarchaeology: Methods, applications, and recent trends, J. Archaeol. Sci. Rep. 18 (2018) 806–823, https://doi.org/10.1016/j.jasrep.2017.12.029.
[20] B.J. Bulkin, The Raman effect: an introduction, in: J.G. Grasselli, B.J. Bulkin (Eds.), Analytical Raman Spectroscopy, John Wiley & Sons, New York, 1991, pp. 1–19.
[21] A. del Amo, García, J.S. de Oliveira, B. Pritchard, D. Walsh, Section one – the sensitive layers - support and emulsion classification, Film Preserv. F.I.A.F. (2004) 105–106.
[22] M.R. Huang, X.G. Li, Thermal degradation of cellulose and cellulose esters, J. Appl. Polym. Sci. 68 (1998) 293–304, https://doi.org/10.1002/(SICI)1097-4628(19980411)68:2< 293::AID-APP11> 3.0.CO;2-Z.
[23] M. Ibrahim, A.A. Mahmoud, O. Osman, M. Abd El-Aal, M. Eid, Molecular spectroscopic analyses of gelatin, Spectrochim. Acta A 81 (2011) 724–729, https://doi.org/10.1016/j.saa.2011.07.012.
[24] British Kinematography, vol. 15, n. 5, British Kinematograph Society, London 1949, pp. 171.
[25] P. Wojciechowska, A. Heimowska, Z. Foltynowicz, M. Rutkowska, Degradability of organic-inorganic cellulose acetate butyrate hybrids in sea water, Pol. J. Chem. Technol. 13 (2011) 29–34, https://doi.org/10.2478/v10026-011-0020-y.
[26] M. Nejström, B. Andreasson, J. Sjölund, A. Eivazi, I. Svanedal, H. Edlund, M. Norgren, On structural and molecular order in cellulose acetate butyrate films, Polymers 15 (2023) 2205, https://doi.org/10.3390/polym15092205.
[27] G. Hill, Care of plastic film-based negative collections, CCI Tech. Bull. 35 (2020). ⟨https://www.canada.ca/en/conservation-institute/services/conservation-preservation-publications/technical-bulletins/care-plastic-negative.html#a4b⟩ (accessed 18 May 2025).
[28] M. Djebara, J.P. Stoquert, M. Abdesselam, D. Muller, A.C. Chami, FTIR analysis of polyethylene terephthalate irradiated by MeV He+, Nucl. Instrum. Meth. B. 274 (2012) 70–77, https://doi.org/10.1016/j.nimb.2011.11.022.
[29] Z. Chen, J.N. Hay, M.J. Jenkins, The thermal analysis of poly (ethyleneterephthalate) by FTIR spectroscopy, Thermochim. Acta 552 (2013) 123–130, https://doi.org/10.1016/j.tca.2012.11.002.
[30] G.C. Inskeep, P.Van Horn, Cellophane, Ind. Eng. Chem. 44 (1952) 2511–2524, https://doi.org/10.1021/ie50515a016.
[31] C. Thielemann, An exploratory study on the physical properties of Ozaphan-films", Cent. Sper. di Cinematogr. (2022) 18–19.
[32] C. Zhou, G. Han, S. Gao, M. Xing, Y. Song, W. Jiang, Rapid determination of cellulose content in pulp using near infrared modeling technique, BioResources 13 (2018) 6122–6132, https://doi.org/10.15376/biores.13.3.6122-6132.
[33] M. Schwanninger, J.C. Rodrigues, K. Fackler, A review of band assignments in near infrared spectra of wood and wood components, J. Infrared Spectrosc. 19 (2011) 287–308, https://doi.org/10.1255/jnirs.955.
[34] F. Zapata, M. Ferreiro-González, C. García-Ruiz, Interpreting the near infrared region of explosives, Spectrochim. Acta A. 204 (2018) 81–87, https://doi.org/10.1016/j.saa.2018.06.002.
[35] K.B. Beć, J. Grabska, J. Badzoka, C.W. Huck, Spectra-structure correlations in NIR region of polymers from quantum chemical calculations. The cases of aromatic ring, C= O, C≡ N and C-Cl functionalities, Spectrochim. Acta A. 262 (2021) 120085, https://doi.org/10.1016/j.saa.2021.120085.
[36] Chemical Book, Triphenyl phosphate (115-86-6) Raman, ⟨https://www.chemicalbook.com/SpectrumEN_115-86-6_Raman.htm⟩, 2017 (Accessed 3 February 2025).
[37] K. Zhang, A. Feldner, S. Fischer, FT Raman spectroscopic investigation of cellulose acetate, Cellulose 18 (2011) 995–1003, https://doi.org/10.1007/s10570-011-9545-8.
[38] J.A. Sánchez-Márquez, R. Fuentes-Ramírez, I. Cano-Rodríguez, Z. Gamiño-Arroyo, E. Rubio-Rosas, J.M. Kenny, N. Rescignano, Membrane made of cellulose acetate with polyacrylic acid reinforced with carbon nanotubes and its applicability for chromium removal, Int. J. Polym. Sci. (2015) 320631, https://doi.org/10.1155/2015/320631.
[39] K.C. Högström, H. Lundgren, S. Wilken, T.G. Zavalis, M. Behm, K. Edström, P. Jacobsson, P. Johansson, G. Lindbergh, Impact of the flame retardant additive triphenyl phosphate (TPP) on the performance of graphite/LiFePO4 cells in high power applications, J. Power Sources 256 (2014) 430–439, https://doi.org/10.1016/j.jpowsour.2014.01.022.
[40] E. Rebollar, S. Pérez, M. Hernández, C. Domingo, M. Martín, T.A. Ezquerra, J. P. Garcìa-Ruiz, M. Castillejo, Physicochemical modifications accompanying UV laser induced surface structures on poly(ethyleneterephthalate) and their effect on adhesion of mesenchymal cells, Phys. Chem. Chem. Phys. 16 (2014) 17551–17559, https://doi.org/10.1039/C4CP02434F.
[41] A.A. Karpenko, V.S. Odintsov, Assessment of microplastic degradation in bottom sediments using raman microspectroscopy and atomic force microscopy, Russ. J. Mar. Biol. 49 (2023) 251–258, https://doi.org/10.1134/S1063074023040053.
[42] M. Ducci, Diazotype–a historical copying process, World J. Chem. Educ. 9 (2021) 136–143, https://doi.org/10.12691/wjce-9-4-6.
[43] P.K. Bajpai, B. Pal, T.B. Baul, Structure of some arylazophenols and arylazonaphthols in the solid state: a resonance Raman study, J. Raman Spectrosc. 26 (1995) 217–222, https://doi.org/10.1002/jrs.1250260303.
[44] W.W. Chin, The partial least squares approach for structural equation modeling, in: G.A. Marcoulides (Ed.), Modern Methods for Business Research, Lawrence Erlbaum Associates Publishers, Mahwah (NJ, USA), 1998, pp. 295–336.
[45] Eastman Kodak Company, History of 16mm, ⟨https://www.kodak.com/en/motion/page/100-years-of-16mm-film/⟩, 2025 (Accessed 13 February 2025).
[46] Eastman Kodak Company, Super 8mm History, ⟨https://www.kodak.com/en/motion/page/super-8-history/⟩, 2025 (Accessed 13 February 2025).
[47] Harpers Ferry Center, History of Film Types Timeline, ⟨https://www.nps.gov/subjects/hfc/history-of-film-types-timeline.htm⟩ (Accessed 13 February 2025).